

Analysis of Chilled Water Storage Integration in Air Conditioning Systems for Dynamic PV Self-Consumption[#]

Wanfang Zhao¹, Jinqing Peng^{1,2*}, Jingyu Cao^{1,2}

1 College of Civil Engineering, Hunan University, Changsha, 410082, China

2 Key Laboratory of Building Safety and Energy Efficiency of Ministry of Education, Hunan University, Changsha, 410082, China
(Corresponding Author: jqpeng@hnu.edu.cn)

ABSTRACT

Chilled water storage is commonly employed in centralized cooling systems for peak shaving, demonstrating significant potential of load flexibility. However, this cost-effective and accessible flexibility resource has seldom been integrated into domestic air-conditioning systems in response to dynamic electricity tariffs or photovoltaic (PV) generation. This paper focused on capacity design and performance evaluation of air-conditioning systems integrated with chilled water storage for improving PV self-consumption in domestic applications. Operation strategies involving temperature control and flow rate control were both considered. The results show that chilled water storage presents an annual cost saving of over 10% and significantly improves PV self-consumption compared to the baseline case without storage. Furthermore, the chilled water storage shows its additional advantage over the battery system in reducing the capacity of the chiller from 7.5 kW to 6.7 kW and enhancing energy efficiency of the air-conditioning with an average COP increasing from 2.87 to 3.14.

Keywords: chilled water storage, demand-side management, optimal design, residential buildings, partial-load efficiency

1. INTRODUCTION

The rapid growth of distributed photovoltaic (PV) technology [1] has introduced significant operation uncertainty and burdens to the utility grid [2]. Given that building operation constitutes 30% of global energy use [3], integrating an energy storage system in demand-side management is essential to balance electricity supply and demand [4].

With the high cost of electric batteries, thermal energy storage (TES) offers a cost-effective alternative for domestic demand-side management [5], transferring

from a mere peak shaving tool [6]. Studies have demonstrated that integrating TES with heating systems, such as a water tank or borehole TES, could achieve solar contribution of up to 50% [7]. Ice storage in PV-driven air-conditioner also significantly improves PV self-consumption rate and reduces electricity cost by up to 30% [8]. Despite the broad adoption of TES, most research has focused on heating applications [9], leaving the potential of cold storage for PV self-consumption unexplored. Moreover, the impacts of TES integration on the performance of a heating, ventilation, and air-conditioning system (HVAC) needs to be explored.

This study examines the optimal design and overall PV utilization performance of chilled water storage (CWS) in an HVAC system. It compares temperature control and flow rate control strategies for the CWS with the maximizing self-consumption strategy by using battery systems [10], aiming to provide a comprehensive understanding of CWS's role in PV self-consumption and HVAC system performance.

2. METHODOLOGY

2.1 System description

As an alternative to electric energy storage, the CWS was adopted for real-time power modulation and PV utilization. The conceptual framework of the proposed PV self-consumption approach is illustrated in Fig. 1. The system mainly comprises PV modules, the main unit of a water-based air-conditioning system, and a CWS integrated into the HVAC system. Upon receiving a power regulation signal from the energy management system (EMS), the CWS dynamically adjusts the chiller's cooling capacity by either charging or discharging the stored chilled water. This process enables cooling demand regulation to align with available PV power. The management of the CWS can be achieved through temperature control, by adjusting the setpoint of the

[#] This is a paper for the 16th International Conference on Applied Energy (ICAE2024), Sep. 1-5, 2024, Niigata, Japan.

storage temperature, or through flow rate control, by regulating the valves within the water tank loop.

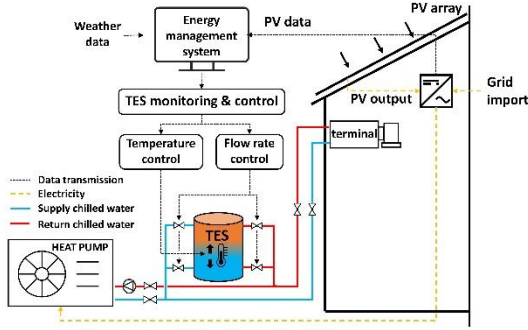


Fig. 1 Schematic diagram of the TES-integrated system

2.1.1 PV model

The PV power generation was calculated using a typical efficiency model [11] expressed in Eq. (1-2). The PV output was calculated using the solar irradiance I_t^g , PV array area A , the PV generation efficiency under standard test condition (STC) η^{STC} , the inverter efficiency η^{inv} , and the power loss coefficient η_T . η_T was derived from the temperature coefficient of power γ , and the cell temperature at present and STC, respectively.

$$P_t^{PV} = I_t^g \times A \times \eta^{STC} \times \eta^{inv} \times \eta_T \quad (1)$$

$$\eta_T = 1 + \gamma \times (T_t^{module} - T^{STC}) \quad (2)$$

2.1.2 Building thermal model

A four-room building located in Changsha, China, was investigated in this work. Changsha is characterized with a hot summer and cold winter climate. The air-conditioning thermal demand of the building was calculated using a validated model built in Modelica platform. The hourly cooling demand through the whole cooling season (from 15th May to 15th Oct.) was calculated by setting the indoor temperature setpoint of 26 °C and all-day operation, as shown in Fig. 2.

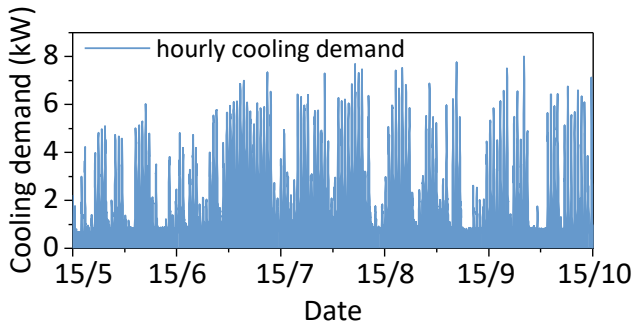


Fig. 2 Hourly cooling demand through cooling season

2.1.3 Air-cooled chiller model

The EIR chiller model was adopted for an air-cooled chiller, which uses three performance curves to determine the chiller operation under a certain temperature and partial-load condition, and is expressed as follows [12]:

$$CAPFT = a_0 + a_1 T_t^{cw,l} + a_2 (T_t^{cw,l})^2 + a_3 T_t^{cond,e} + a_4 (T_t^{cond,e})^2 + a_5 T_t^{cw,l} T_t^{cond,e} \quad (3)$$

$$EIRFT = b_0 + b_1 T_t^{cw,l} + b_2 (T_t^{cw,l})^2 + b_3 T_t^{cond,e} + b_4 (T_t^{cond,e})^2 + b_5 T_t^{cw,l} T_t^{cond,e} \quad (4)$$

$$EIRFPLR = c_0 + c_1 PLR_t + c_2 (PLR_t)^2 \quad (5)$$

where $T_t^{cw,l}$ is the supplied chilled water temperature, $T_t^{cond,e}$ is the outside air temperature, PLR_t is the part load ratio of the chiller.

2.1.4 Chilled water storage model

For the flow rate control strategy, a stratified water tank model was developed. The energy storage condition was expressed by the volume and temperature of the upper layer (storing return chilled) and bottom layer (storing supply chilled water). Taking the upper layer as an example, the volume and temperature can be updated using the following equations:

$$m_t^{up} = m_{t-1}^{up} + (\dot{m}_t^{dis} - \dot{m}_t^{ch}) \times \Delta t \quad (7)$$

$$T_t^{up} = \frac{c_p \dot{m}_t^{dis} T_t^{re} - c_p \dot{m}_t^{ch} T_t^{re} + Q_t^{loss} + c_p m_{t-1}^{up} T_{t-1}^{up}}{c_p m_t^{up}} \quad (8)$$

where m_t^{up} and T_t^{up} are the mass and the temperature of the upper layer, \dot{m}_t^{ch} and \dot{m}_t^{dis} are the charging and discharging mass flow rates, respectively, T_t^{re} is the chilled water return temperature of chiller, c_p is the heat capacity of the chilled water, Q_t^{loss} is the heat loss of the CWS.

For the temperature control strategy, an identical water tank was adopted. The storage condition was only characterized by the temperature change of the stored water using the following equation:

$$c_p m_t^{TES} (T_t^{TES} - T_{t-1}^{TES}) = (Q_t^{ch} \times \eta^{TES} - Q_t^{dis} / \eta^{TES}) \times \Delta t + Q_t^{loss} \quad (9)$$

where η^{TES} is the storage efficiency of the CWS, Q_t^{ch} and Q_t^{dis} are the charging and discharging heat flow rates, respectively.

2.2 Control strategy and energy management

The CWS typically employs a temperature control strategy, where the setpoint of the water tank is adjusted to modulate power consumption. The method is particularly suitable for domestic applications due to its simplicity and compatibility with existing air conditioning systems, making it easier to integrate into an automated

control. On the other hand, a flow rate control strategy, which directly alters the chilled water distribution between the main unit and the CWS, offers more precise and direct regulation of the charging and discharging rates. However, this approach is more complex to control and requires additional devices for flow monitoring and adjustment. Given the potential benefits of both strategies, they were both considered in this study.

Figure 3 illustrates the control flow charts of the two strategies. Under the temperature control, the temperature setpoint of the CWS is lowered when the PV output exceeds a predetermined charging threshold. Conversely, the chiller shuts down and CWS discharges when the PV output falls below the discharging threshold. In the flow rate control strategy, it is regarded that various charging and discharging rates can be achieved through flexible flow rate adjustment, allowing the chiller to operate in alignment with PV power generation. It is noted that in both strategies, cold discharging is activated if cooling demand is not met.

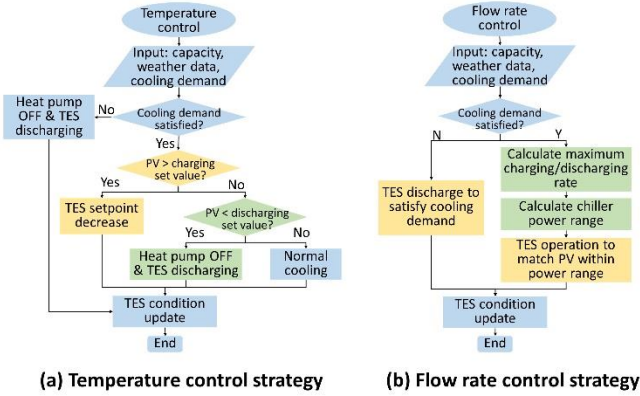


Fig. 3 TES control strategies

2.3 Optimization framework

To evaluate different PV self-consumption approaches, optimization is essential to obtain their optimal capacities and performance for comparison. The optimization framework is outlined in the following sub-sections.

2.3.1 Decision variables

In this study, CWS integration with both temperature and flow rate control was considered and compared against the traditional electricity energy storage (EES) scenario and the baseline scenarios without any energy storage. In the EES-integration scenario, a typical battery model and a traditional MSC strategy were adopted as described in Ref. [10].

The input parameters include meteorological data (T_r^{amb} , I_r^g) and the building's cooling demand Q_i^{de} . The

decision variables for both the CWS and the battery cases comprise the total installed PV capacity E^{PV} , the rated cooling capacity of chiller $Q^{c, rated}$, and the thermal or electrical storage capacity. For a more intuitive analysis of capacities, the installed PV capacity and storage capacity were normalized by the total HVAC energy consumption during cooling season and by the design day cooling load, respectively [13].

2.3.2 Objective functions and constraints

The objective function was set to minimize the annual cost (C^{annual}), including the annualized capital cost ($C^{capital}$), and the annual operation cost (C^{grid}), which is expressed as follows [14]:

$$\min C^{annual} = \min(C^{capital} + C^{grid}) \quad (10)$$

$$C^{capital} = \sum_{i=1}^n C_i \frac{r(1+r)^{Y_i}}{(1+r)^{Y_i} - 1} \quad (11)$$

$$C^{grid} = \sum_{t=1}^{t^{cooling}} c_t^{grid} P_t^{grid} \quad (12)$$

where C_i and Y_i are the capital cost and lifetime of each component, r is the interest rate (4%), $c_{grid}(t)$ is the electricity prices as illustrated in Fig. 4.

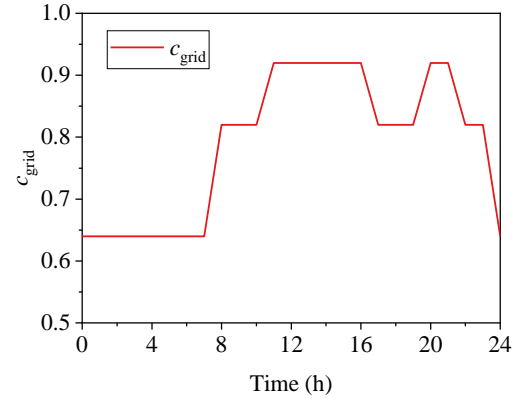


Fig. 4 Time-of-Use tariff

The constraints in this optimization problem were listed as follows:

$$0 \leq Q_i^c < Q^{avail} \quad (13)$$

$$0 \leq m_t^{up} \leq m^{TES} \quad (14)$$

$$0 \leq m_t^b \leq m^{TES} \quad (15)$$

$$5^\circ\text{C} \leq T^{TES} \leq 12^\circ\text{C} \quad (16)$$

$$1 - DOD^{EES} \leq SOC_t^{EES} \leq 100\% \quad (17)$$

$$abs(P_t^{EES}) \leq \frac{1}{2} E^{EES} \quad (18)$$

where Q^{avail} is the available cooling capacity of the chiller, DOD^{EES} is the maximum depth of discharging

of the EES, DOD^{EES} is the state of charging of the EES at the time step t , P_t^{EES} is the charging or discharging power of the battery.

In this study, the time interval was set as 1h during the optimization horizon of the whole cooling season. The particle swarm optimization algorithm was used to solve the problem.

2.4 Performance evaluation

The performance of each PV self-consumption approach was evaluated from the following aspects:

(1) Cost saving, which is calculated using the following equation:

$$EnergySaving(\%) = \frac{C^{annual} - C^{annual,base}}{C^{annual,base}} \times 100\% \quad (19)$$

(2) PV self-consumption, which is evaluated as follows and compared with total grid import electricity:

$$SC = \sum_{t=1}^{t=t_{cooling}} \min(P_t^{PV}, P_t^c) \Delta t \quad (20)$$

(3) Load shifting index (LSI), which is calculated as follows [9]:

$$LSI = \frac{\frac{eu^{offpeak}}{t^{offpeak}} - \frac{eu^{peak}}{t^{peak}}}{\frac{eu^{offpeak}}{t^{offpeak}} + \frac{eu^{peak}}{t^{peak}}}} \times 100\% \quad (22)$$

where eu^{peak} and $eu^{offpeak}$ are the energy consumption during peak and off-peak periods, respectively, t^{peak} and $t^{offpeak}$ are the duration of peak and off-peak periods, respectively.

(4) The average coefficient of efficiency (COP) of the chiller is calculated as follows:

$$COP = \frac{\sum_{t=1}^{t=t_{cooling}} Q_t^c}{\sum_{t=1}^{t=t_{cooling}} P_t^c} \quad (23)$$

3. RESULTS AND DISCUSSION

3.1 Optimal design comparison between different approaches

This section evaluated the capacities and performance of different PV self-consumption approaches. The optimal capacities between the electrical storage and the cold storage of different control strategies are displayed in Fig. 5. The storage capacity in the EES integration scenario is only 13% due to the high cost of the batteries, highlighting the cost advantage of the chilled water storage. This demonstrates that a large chilled water tank can be

installed at a limited capital cost, making it an appealing option for homeowners who prefer more cost-effective solutions. CWS integration with temperature control strategy also presented a lower energy storage of 11% compared to 22% in the flow rate control scenario. This difference can be explained by the daily operation patterns of different energy storage approaches, as illustrated in Fig. 6. For the temperature control strategy, charging is activated according to a fixed threshold, and the chiller generally operates at full load at the beginning of charging to reach the updated setpoint. Consequently, the chiller power can exceed the PV output during charging, such as 8:00-10:00 on Day 1, leading to additional grid imports. As a result, a low CWS capacity is designed to reduce this undesirable operation costs. In contrast, Fig. 6 (c) shows that flow rate control achieves better PV tracing, especially between 8:00-10:00 and 16:00-18:00. The flexible flow rate adjustment allows the chiller's cooling demand to be regulated more precisely. Therefore, CWS with flow rate control proves to be a superior alternative to batteries in PV utilization compared to temperature control.

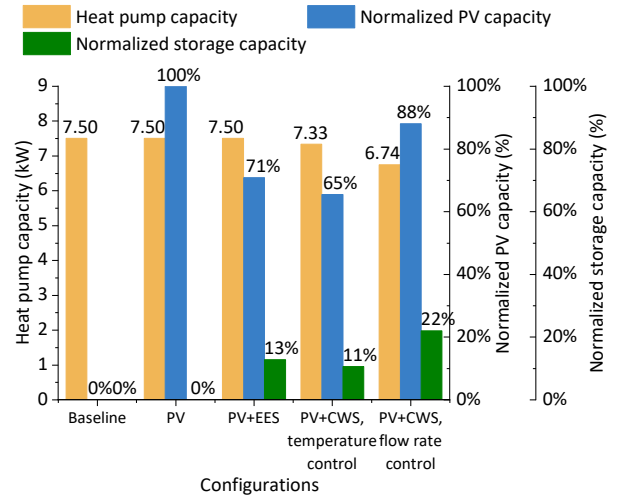


Fig. 5 Optimal capacities of different configurations

The optimal PV and chiller capacities also vary between different approaches. With similar energy storage results, the EES integration case and CWS with temperature control strategy exhibit similar PV capacities. However, the PV capacity is significantly higher in the flow rate control strategy. This is attributed to the reduced chiller capacity. It can be seen from Fig. 6 (c) that the peak cooling load can be shaved by cold discharging through flow rate adjustment. Hence, the cooling capacity of the chiller can be reduced to 6.74 kW compared to 7.5 kW in the baseline case. To store enough cold energy for peak load shaving, an increased

PV capacity is necessary. This accounts for the normalized PV capacity of 88% in the flow rate control strategy. The results highlight the advantage of reducing the cooling capacity of the air-conditioning system by using TES, especially the flow rate control strategy.

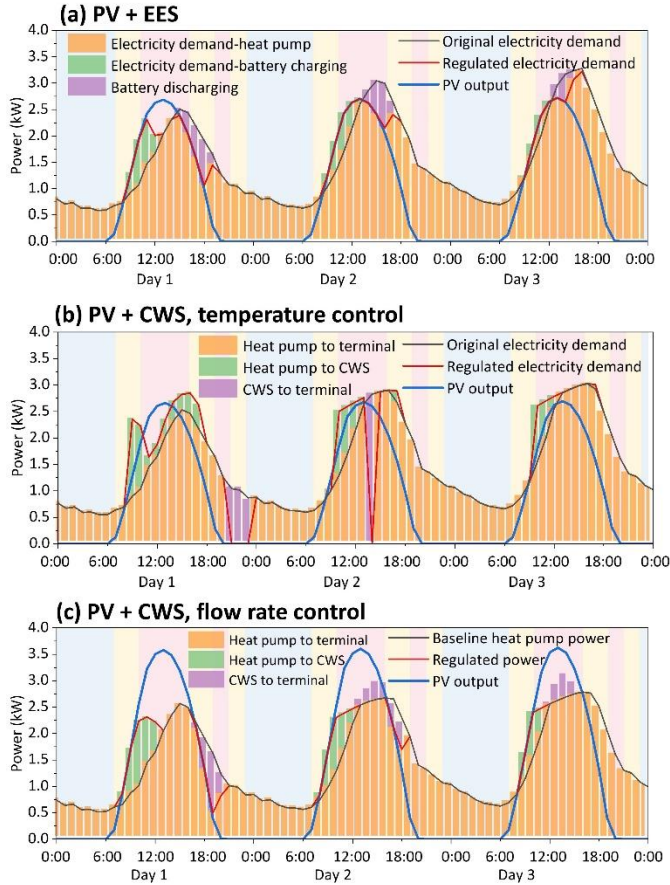


Fig. 6 Daily operation of different energy storage approaches

3.2 Overall performance comparison between different approaches

Fig. 7 shows the performance evaluation of different approaches. Fig. 7 (a) shows the annual costs of using different approaches. Energy storage achieves cost savings of at least 9%, despite higher capital costs than the baseline case. The CWS, in particular, provides significant cost savings, with values of 10.1% and 14.8%. Comparing different CWS strategies, Fig. 7 (b) reveals that temperature control causes a high operation cost due to the additional grid import during Day charging. In contrast, flow rate control exhibits a low operation cost and energy consumption. This is attributed to the better PV tracking and the improved energy efficiency with flow rate control. As shown in Fig. 7 (c), the CWS-integrated HVAC systems can deliver a higher COP, as the cooling load can be shifted from peak periods to the times with

lower environmental temperatures. For example, under the flow rate control, part of the cooling demand from 16:00 to 18:00 on Day 1 was shifted to the morning period between 7:00 and 11:00. Hence, the efficiency of the chiller can be enhanced by avoiding operation at high environmental temperature, leading to a high average COP of 3.14.

The demand flexibility was assessed using the load shifting index (LSI). LSI shows the percentage of load consumed during peak periods, thus a lower LSI is more preferable. Integrating PV or energy storage can improve the LSI by reducing grid imports during the peak hours of 11:00-16:00. However, the LSI is only 0.19 under TES temperature control, as cold charging may be activated even during peak hours as long as the PV output exceeds the threshold, leading to undesirable grid imports and increased operation cost.

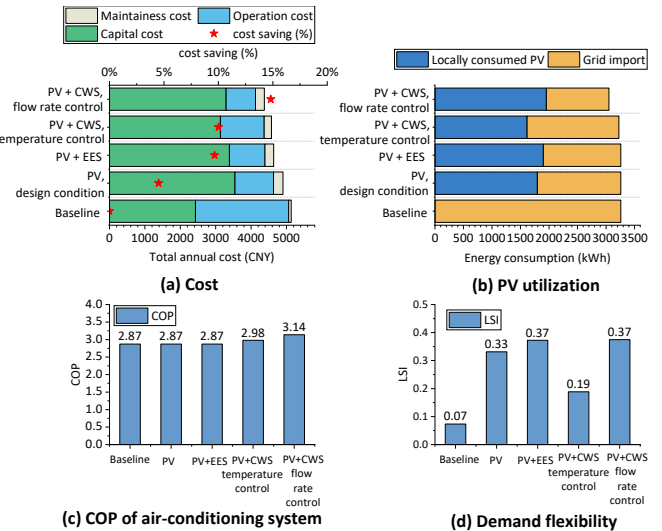


Fig. 7 Performance evaluation of different energy storage approaches

4. CONCLUSIONS

This study explored the optimal design and overall performance of chilled water storage as an alternative to electrical energy storage for PV self-consumption in residential buildings. Two control strategies for chilled water storage (CWS), viz. temperature control and flow rate control, were investigated and compared with the traditional battery integration scenario. The results demonstrated that the CWS provides a significant cost advantage, achieving annual cost savings of over 10%. Particularly, CWS with flow rate control could achieve similar PV tracking performance to the electrical energy storage system but at a lower capital cost. Additionally, the CWS effectively achieved peak cooling load shaving. This highlights the advantage of thermal energy storage

in enhancing energy efficiency and reducing the rated capacity of air-conditioning systems.

Further research will explore the adoption of cold energy for PV utilization in more scenarios, such as different climates and PV penetration levels. Furthermore, optimal scheduling strategies, with multiple objectives, for CWS application will be considered. This will provide general guidance for homeowners with different requirements.

ACKNOWLEDGEMENT

This work was supported by the National Natural Science Foundation of China [grant numbers 52278104], and the Science and Technology Innovation Program of Hunan Province [grant number 2023RC1042].

REFERENCE

[1] International Energy Agency. (2024, July 25) *Solar - IEA*. Retrieved from <https://www.iea.org/energy-system/renewables/solar-pv#tracking>

[2] Rahdan P, Zeyen E, Gallego-Castillo C, Victoria M. Distributed photovoltaics provides key benefits for a highly renewable European energy system. *Appl. Energy* 2024;360:122721. <https://doi.org/10.1016/j.apenergy.2024.122721>

[3] International Energy Agency. (2024, July 25) *World Energy Outlook 2023*. Retrieved from <https://www.iea.org/news/the-energy-world-is-set-to-change-significantly-by-2030-based-on-today-s-policy-settings-alone>

[4] Nawaz A, Wu J, Ye J, Dong Y, Long C. Distributed MPC-based energy scheduling for islanded multi-microgrid considering battery degradation and cyclic life deterioration. *Appl. Energy* 2023;329:120168. <https://doi.org/10.1016/j.apenergy.2022.120168>

[5] Odukomaiya A, Woods J, James N, Kaur S, Gluesenkamp KR, Kumar N et al. Addressing energy storage needs at lower cost via on-site thermal energy storage in buildings. *Energy Environ. Sci.* 2021;14:5315–5329. <https://doi.org/10.1039/D1EE01992A>

[6] Liu Z, Chen Y, Yang X, Yan J. Power to heat: Opportunity of flexibility services provided by building energy systems. *Adv. Appl. Energy* 2023;11:100149. <https://doi.org/10.1016/j.adapen.2023.100149>

[7] Berger M, Schroeteler B, Sperle H, Püntener P, Felder T, Worlitschek J. Assessment of residential scale renewable heating solutions with thermal energy storages. *Energy* 2022;244:122618. <https://doi.org/10.1016/j.energy.2021.122618>

[8] Xu B, Li M, Hassanien RHE, Zhang Y, Wang Y, Xu Q et al. Research on the Cold Storage Characteristics of Ice Storage Photovoltaic Cold Storage. *Energy Built Environ.* 2024:0–27. <https://doi.org/10.1016/j.enbenv.2024.03.011>

[9] Yang S, Gao HO, You F. Demand flexibility and cost-saving potentials via smart building energy management: Opportunities in residential space heating across the US. *Adv. Appl. Energy* 2024;14:100171. <https://doi.org/10.1016/j.adapen.2024.100171>

[10] Zou B, Peng J, Li S, Li Y, Yan J, Yang H. Comparative study of the dynamic programming-based and rule-based operation strategies for grid-connected PV-battery systems of office buildings. *Appl. Energy* 2022;305:117875. <https://doi.org/10.1016/j.apenergy.2021.117875>

[11] Wang M, Peng J, Luo Y, Shen Z, Yang H. Comparison of different simplistic prediction models for forecasting PV power output: Assessment with experimental measurements. *Energy* 2021;224:120162. <https://doi.org/10.1016/j.energy.2021.120162>

[12] Hydeman, M. and K.L. Gillespie. Tools and Techniques to Calibrate Electric Chiller Component Models. *ASHRAE Transactions* 2002;108:733-741.

[13] Chen Q, Kuang Z, Liu X, Zhang T. Optimal sizing and techno-economic analysis of the hybrid PV-battery-cooling storage system for commercial buildings in China. *Appl. Energy* 2024;355:122231. <https://doi.org/10.1016/j.apenergy.2023.122231>

[14] Zang X, Li H, Wang S. Optimal design of energy-flexible distributed energy systems and the impacts of energy storage specifications under evolving time-of-use tariff in cooling-dominated regions. *J. Energy Storage* 2023;72:108462. <https://doi.org/10.1016/j.est.2023.108462>